

Response Acceleration in Post-translationally Regulated Genetic Circuits

Alexander Y. Mitrophanov and Eduardo A. Groisman*

Howard Hughes Medical Institute, Department of Molecular Microbiology, Washington University School of Medicine, Campus Box 8230, 660 South Euclid Avenue, St. Louis, MO 63110, USA

Received 1 October 2009;
received in revised form
28 October 2009;
accepted 16 November 2009
Available online
20 November 2009

Transcription factors must often be chemically modified to perform their functions. Yet, it is not known whether the mechanisms that bring about such modifications impact the quantitative or kinetic properties of gene expression. Phosphorylation controls the activity of regulatory proteins of the two-component system family, which constitutes a prevalent form of bacterial signal transduction. These proteins are phosphorylated/dephosphorylated by cognate sensor proteins in response to specific signals. The phosphorylation level of the regulatory proteins is also modulated by small proteins—termed connectors—that are produced when a cell experiences signals other than those detected directly by the sensors. Here, we explore how differences in the targets (i.e., sensor or regulator) and the mechanisms used by connectors to generate phosphorylated regulatory proteins affect the output of two-component systems. Our mathematical modeling demonstrates that sensor-targeting mechanisms exhibit stronger response acceleration than those where the connector targets the regulator. These differences are robust to perturbations in kinetic parameters but dependent upon the specific sensor-to-regulator ratio and how the ratio is controlled in living cells. In contrast, the steady-state output levels of the circuits are determined primarily by the circuit parameters, and can be adjusted without affecting response acceleration. Likewise, the analyzed connector-mediated circuits exhibit similar noise generation properties. Our results highlight the relationship between the architecture of genetic regulatory circuits and their dynamic properties.

© 2009 Elsevier Ltd. All rights reserved.

Edited by B. Honig

Keywords: dynamics; mathematical modeling; phosphorylation; signal transduction; two-component systems

Introduction

Transcription factors (TFs) typically require a chemical decoration to perform their functions. For example, phosphorylation can promote TF dimerization, enhance the affinity of a TF for its binding sites, and/or its ability to recruit RNA polymerase.^{1–4} In two-component regulatory systems (TCSs), a sensor protein autophosphorylates from ATP and then transfers the phosphoryl group

to a cognate regulator and, in many cases, a sensor displays phosphatase activity towards the phosphorylated regulator.^{4,5} Therefore, the balance of the kinase and phosphatase activities of a sensor determines the level of phosphorylated regulator and, thus, the expression output of its regulated genes because the vast majority of regulators are TFs that are active only in their phosphorylated state *in vivo*.⁶ TCSs are widely used by bacteria, fungi, and plants to modulate gene expression in response to extra- or intracellular stimuli. Many TCSs are feedback-regulated such that the phosphorylated regulator positively⁷ or negatively⁸ controls transcription of the corresponding sensor and regulator genes.

The degree of phosphorylation of a regulator can be influenced by signals not detected directly by its cognate sensor. In this case, TCS connector proteins (also referred to as connectors) target a sensor or a regulator, thereby changing the level of phosphory-

*Corresponding author. E-mail address: groisman@borcim.wustl.edu.

Present address: A. Y. Mitrophanov, Biotechnology High-Performance Computing Software Applications Institute (BHSAI), 2405 Whittier Drive, Suite 200, Frederick, MD 21702, USA.

Abbreviations used: TF, transcription factor; TCS, two-component regulatory system.

lated regulator and/or its ability to regulate gene expression (e.g., by preventing the interaction of a regulator with DNA).³ Connectors enable signal integration by virtue of being made under conditions other than those detected by the sensor proteins. For example, the connector PmrD protein from *Salmonella enterica* binds to the phosphorylated form of the regulator PmrA and hinders its dephosphorylation by the PmrA cognate sensor PmrB;⁹ this is reminiscent of the eukaryotic 14–3–3 family of post-translational regulators.¹⁰ This allows PmrA-activated genes to be expressed when *S. enterica* experiences Fe³⁺, which is a signal detected by PmrB,¹¹ and in low Mg²⁺, which is a condition promoting transcription of the *pmrD* gene.¹² Likewise, the B1500 protein from *Escherichia coli* binds to the sensor protein PhoQ, resulting in enhanced expression of genes activated by the PhoQ cognate regulator PhoP.¹³

Earlier, we established that the PmrD-mediated circuit exhibits quantitative properties distinct from those of a circuit in which a gene is controlled directly by a TF.^{14,15} For instance, expression persistence (i.e., the ability to maintain high output levels after an activating signal disappears) characterizes the post-translational PmrD-mediated circuits with either cascade^{3,14,15} or feedforward^{3,14,15} architectures, which are typically stronger than those exhibited by classical transcriptional cascades and feedforward loops.^{16,17} Expression persistence could potentially contribute to the ability of a bacterial species to survive in fluctuating environments. The critical role of circuit architecture is illustrated by the dramatic disparity in a pathogen's ability to cause disease exhibited by two isogenic *S. enterica* strains that utilize different circuit architectures to achieve the same steady-state levels of expression.¹⁸

Here, we explore how the kinetic properties of regulatory circuits vary depending on the mechanisms utilized by connector proteins to produce and/or maintain the levels of phosphorylated regulator. Our mathematical modeling suggests that sensor-targeting circuits are typically deactivated faster (i.e., they exhibit less expression persistence) than regulator-targeting circuits when the sensor-to-regulator ratio is controlled at the level of protein degradation. This dynamic feature, which we term response acceleration, is robust to perturbations in the circuits' kinetic parameters, but critically dependent on the sensor-to-regulator ratio. By contrast, the steady-state output levels of sensor- and regulator-targeting circuits depend strongly on the values of the kinetic parameters, and can be adjusted without disruption of response acceleration. These results raise the possibility of evolution fine-tuning the output of connector-mediated circuits without interfering with its principal characteristic—deactivation response timing—determined by the mechanism of action of the connector protein. Our predictions may guide the design of synthetic genetic regulatory architectures with specific response rates and levels.

Results

Regulatory circuit models

We used mathematical modeling to analyze the dynamics of connector-mediated circuits so as to zero in on the conceptual differences between regulatory mechanisms (as opposed to their implementations in particular organisms and/or physiological contexts). The analysis focuses on system behavior averaged over a population of genetically identical cells, which allows us to obtain results directly comparable with the quantitative batch-culture measurements for the connector protein PmrD.^{14,15} The models were systems of differential equations derived using the methodology of chemical kinetics (Supporting Data Eqs (1)–(25)). This approach permitted us to study the circuits for a variety of parameter sets, and thus, contributed to the generality of our conclusions.

A connector-mediated circuit consists of a sensor protein, a response regulator, and a connector protein (Fig. 1). The kinase form of the sensor phosphorylates the unphosphorylated response regulator, whereas the phosphatase form dephosphorylates the phosphorylated regulator. We posit that in the absence of its specific signal, the sensor protein is present predominantly in its phosphatase form, which agrees with experimental data for TCSs.⁹ The functional form of the regulator is its phosphorylated form,^{4–6,18} and the level of phosphorylated regulator (including that in complex with a connector protein) is the output of a circuit. Our models reflect that many TCSs feature a positive feedback loop whereby the phosphorylated regulator acts as an activator of transcription of the operon containing both the regulator-and the sensor-encoding genes (Fig. 1).⁷ The connector protein is synthesized from an independently regulated promoter, and its rate of synthesis forms the input of the connector-mediated circuits.

We considered four possible alternative scenarios for the mode of action of connector proteins. In the regulator-protecting circuit, the connector acts by binding to and protecting the phosphorylated form of the regulator from sensor-promoted dephosphorylation (Fig. 1a). We also consider a circuit where the connector binds to the response regulator and stimulates its ability to become phosphorylated by the sensor protein (regulator-activating circuit; Fig. 1b). For sensor-targeting circuits, we evaluated two possibilities: one in which the connector inhibits the sensor's phosphatase activity towards the phosphorylated response regulator (phosphatase-inhibiting circuit; Fig. 1c), and one in which it increases the rate of regulator phosphorylation (kinase-stimulating circuit; Fig. 1d). The first circuit reflects the mode of action of the connector protein PmrD.^{3,14} However, connectors that utilize the other three mechanisms of action have not been identified, yet.

In two-component systems, the level of the regulator protein noticeably exceeds that of the

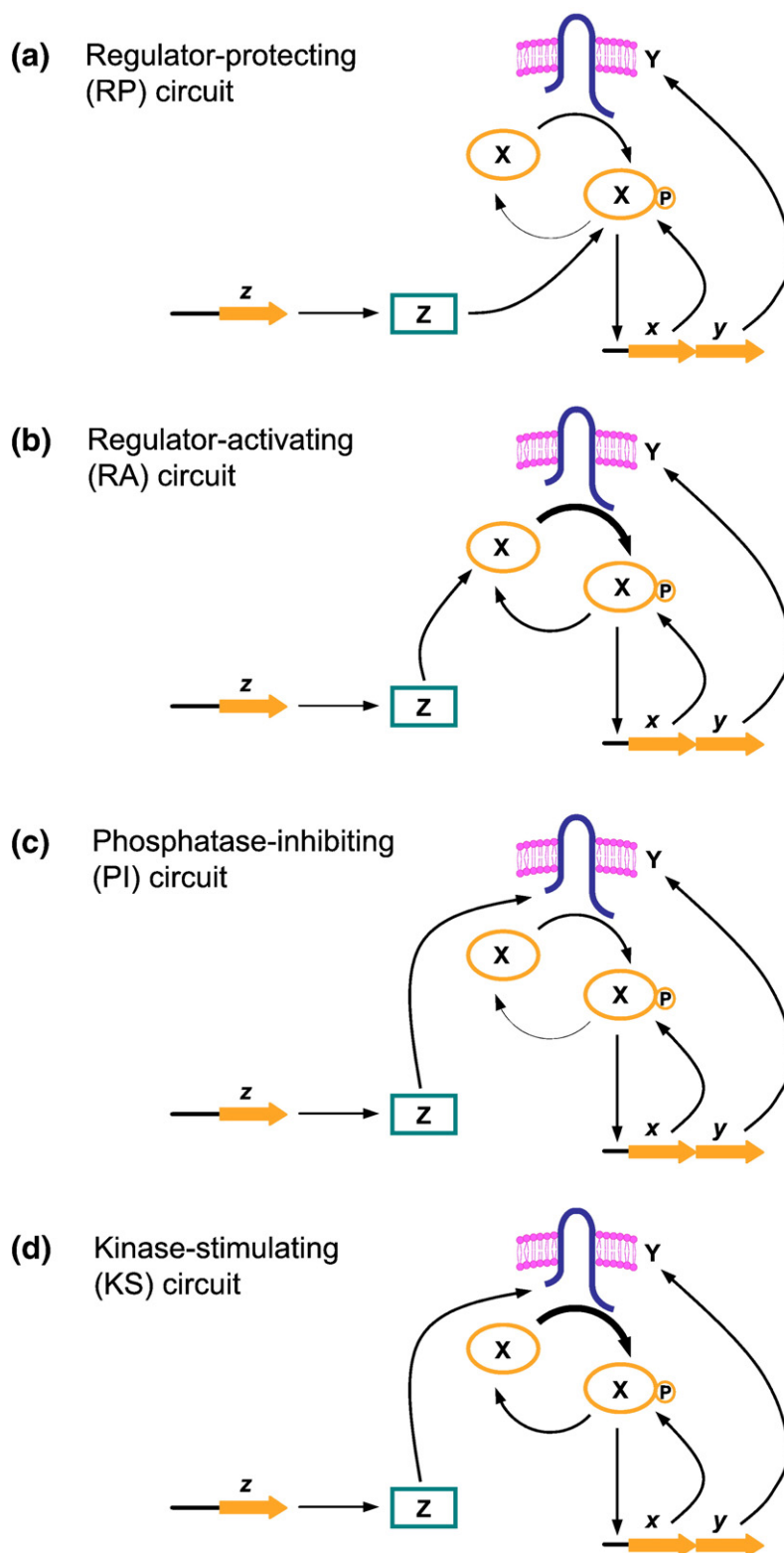


Fig. 1. Regulatory architectures of autoregulated two-component systems that respond to the action of a connector protein. X, response regulator, Y, sensor protein, Z, connector protein; x , y , and z denote the corresponding genes. (a) Regulator-protecting circuit, in which the connector binds to phosphorylated regulator and protects it from dephosphorylation by the sensor protein. (b) Regulator-activating circuit, in which the connector binds to the unphosphorylated regulator and stimulates its phosphorylation by its cognate sensor. (c) Phosphatase-inhibiting circuit, in which the connector binds to the sensor protein and inhibits its phosphatase activity. (d) Kinase-stimulating circuit, in which the connector binds to the sensor protein and stimulates its kinase activity. The relative rates of the response regulator phosphorylation and dephosphorylation processes are indicated by the thickness of the corresponding arrows.

cognate sensor, with reported ratios of 35–50.^{19,20} This could be due to differences in translation efficiency of the corresponding genes, which are typically encoded in polycistronic operons, and/or reflect differential degradation rates of the sensor and regulator proteins. For the sake of simplicity, we initially assumed that the rates of synthesis of sensor and regulator were equal, and focused on the case when the high regulator-to-sensor ratio results from incongruity in their degradation rates. The model considers the degradation rate for the connector–target complex to be equal to that of the unbound target because, to the best of our knowledge, there is no evidence that the stability of sensor or regulator proteins is modified when bound to a connector protein.

Sensor-targeting circuits exhibit response acceleration

We solved the model equations (Supplementary Data Eqs (1)–(25)) numerically for a nominal parameter set (Supplementary Data Table S1), which was chosen using typical values of protein concentrations and lifetimes in signal transduction and gene regulatory circuits.²¹ We calculated the times for the 10% and 50% deactivation thresholds. The 10% deactivation time was defined as the time it takes the circuit output to decrease from its *activated level* to the level:

$$\text{deactivated level} + (\text{activated level} - \text{deactivated level}) / 10$$

and an equivalent definition was used for the 50% deactivation time, except that the divisor 10 was replaced by 2.¹⁵ Of course, the choice of any specific threshold is arbitrary; therefore, by identifying the properties of deactivation response that were present at both the 10% and 50% threshold levels, we hoped to identify timing properties that were independent of specific threshold values.

The sensor-targeting circuits were deactivated much faster than the regulator-targeting circuits at both threshold levels—a phenomenon we termed response acceleration. For example, the 10% deactivation times for the two regulator-targeting circuits exceed 60 min, whereas they are ~10 min for the two sensor-targeting circuits (Fig. 2a). Thus, in the sensor-targeting circuits, the deactivation response is accelerated more than sixfold relative to that of the regulator-targeting circuits.

A positive feedback loop can shape response timing in genetic circuits.^{7,22} Thus, we wondered whether activation and deactivation times would be influenced by the presence of a transcriptional positive feedback loop in the investigated circuits. We examined the behavior of circuits in which positively autoregulated promoters were substituted with constitutive promoters whose strengths were equal to those of the autoregulated promoters under maximal activation conditions. Analysis of such modified circuits is biologically justified because certain connector–modulated TCSs, such as the

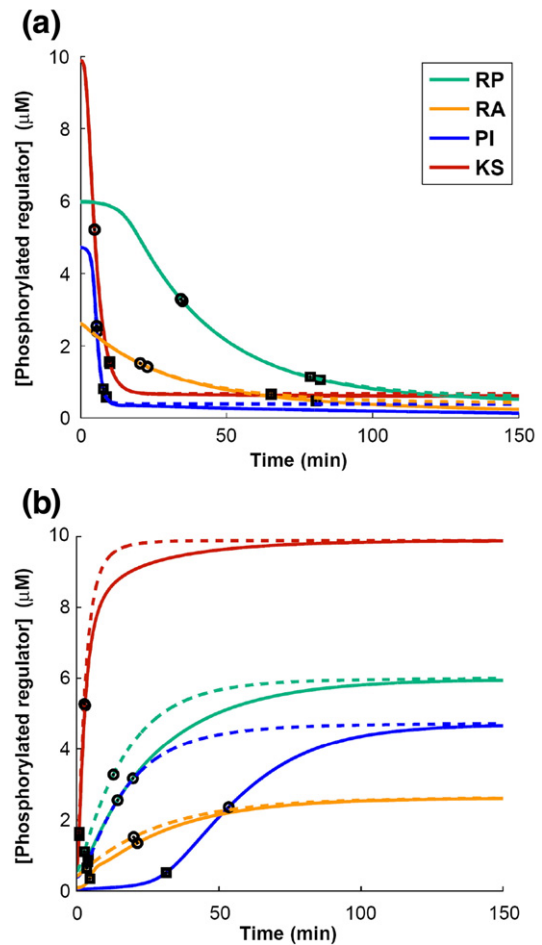


Fig. 2. Dynamic trajectories for the connector-mediated circuits depicted in Fig. 1. (a) Deactivation dynamics. The initial state of the system is its steady state computed for the nominal parameter set (Supplementary Data Table S1), with the connector synthesis rate 50-fold higher. At time zero the connector synthesis rate was decreased 50-fold. (b) Activation dynamics. The initial state of the system is its steady state for the nominal parameter set (Supplementary Data Table S1). At time zero the connector synthesis rate was increased 50-fold. RP, regulator-protecting circuit (Fig. 1a); RA, regulator-activating circuit (Fig. 1b); PI, phosphatase-inhibiting circuit (Fig. 1c); KS, kinase-stimulating circuit (Fig. 1d). Continuous and broken lines correspond to circuits where positive feedback is present and absent, respectively. Filled squares mark the trajectory points that correspond to 10% activation and deactivation times; filled circles mark the points that correspond to 50% activation and deactivation times. Equivalent biochemical parameters had identical values for all four circuits.

ComP/ComA system of *Bacillus subtilis*, do not appear to include a transcriptional feedback loop.²³ Deactivation times were practically unaffected by abrogation of the positive feedback in both the regulator- and sensor-targeting circuits (Fig. 2a).

To examine whether activation times are also insensitive to the presence of positive feedback, we analyzed activation dynamics for the regulator-targeting and sensor-targeting circuits. At both the 10% and 50% threshold levels, the phosphatase-

inhibiting circuit was activated much slower than the regulator-targeting and kinase-stimulating circuits (Fig. 2b). (The 10% activation time is defined as the time it takes the circuit output to increase from its *deactivated level* by the amount:

$$(\text{activated level} - \text{deactivated level}) / 10$$

and an equivalent definition was used for the 50% activation time, except that the divisor 10 was replaced by 2.¹⁵ Removal of positive feedback from the phosphatase-inhibiting circuit accelerated the activation of the phosphatase-inhibiting circuit considerably (Fig. 2b); such an effect is a known property of positive feedback in transcriptionally regulated genetic circuits.²⁴ Cumulatively, our results indicate that positive feedback affects activation time but not deactivation time in connector-mediated circuits.

Response acceleration is robust to changes in the circuit output levels

The specific physiological function of a genetic regulatory circuit often demands that a specific output level be achieved upon activation. This is the reason why comparisons of mathematical models for different circuits are often carried out under equal steady-state output conditions.^{25,26} The regulator-targeting circuits and the sensor-targeting circuits with equivalent parameter sets can generate different output levels (Fig. 2). For example, when the

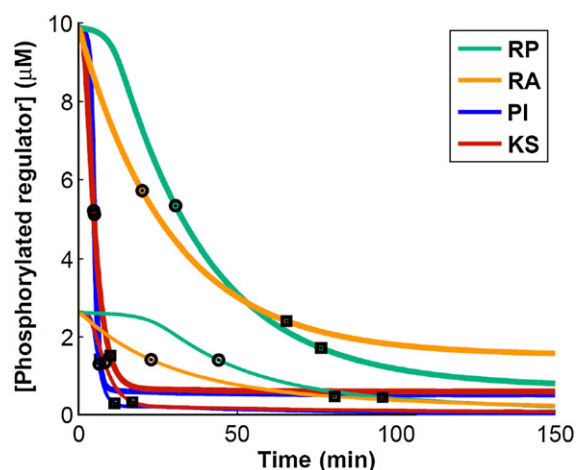


Fig. 3. Deactivation dynamics for the connector-mediated circuits depicted in Fig. 1 with regulator synthesis rates fine-tuned to produce equal activated steady-state levels for all four circuits. All other model parameters retained their nominal values. Deactivation of the system from its activated steady state was performed as in the computational experiment illustrated by Fig. 2a. RP, regulator-protecting circuit (Fig. 1a); RA, regulator-activating circuit (Fig. 1b); PI, phosphatase-inhibiting circuit (Fig. 1c); KS, kinase-stimulating circuit (Fig. 1d). Thick lines, fine-tuning to the highest output level; thin lines, fine-tuning to the lowest output level. Filled squares and circles mark the trajectory points that correspond to 10% and 50% deactivation times, respectively.

connector synthesis rate is high, there is >3-fold difference in the output levels between the sensor-targeting and regulator-targeting circuits (Fig. 2a). Thus, we wished to investigate if the response acceleration displayed by the sensor-targeting circuits during deactivation is preserved when the parameters of the models are adjusted to make the steady-state levels virtually equal.

For the nominal parameter set, the highest steady-state output level upon activation (designated O_1) was achieved by the kinase-stimulating circuit, whereas the lowest steady-state level (O_2) was attained by the regulator-activating circuit (Fig. 2b). By making small adjustments to the rate of regulator synthesis under full activation (which reflects the strength of the autoregulated promoter in the circuits; see details in [Supplementary Data](#)), we fine-tuned the circuit output levels to be nearly equal to either O_1 or O_2 . For both types of adjustments, the sensor-targeting circuits exhibited response acceleration relative to the regulator-targeting circuits (Fig. 3). This result indicates that response acceleration is insensitive to the particular shifts in steady-state output levels, and would still be observed if the circuits were required to generate the same steady-state output level upon activation.

Deactivation response is robust to variations in the connector–target complex formation and dissociation rates

The kinetic parameters that define the interaction of a connector protein with its target (sensor or regulator) are the rate at which the complex between the connector and its target forms and the rate at which it dissociates. To explore whether sensor-targeting circuits still exhibited response acceleration if the parameters governing complex formation and dissociation were significantly different, we performed parameter scans in which these rates were changed by more than two orders of magnitude, and the remaining parameters retained their nominal values. The regulator-targeting circuits were deactivated much more slowly than the sensor-targeting circuits for the vast majority of the considered combinations of complex formation/dissociation rates (Fig. 4a–d). These results suggest that the sensor-targeting circuits will likely demonstrate response acceleration regardless of how strongly a connector protein binds to its target.

The ability of a circuit to increase its output levels in response to a specified increase in the signal intensity is reflected by the activation ratio (i.e., the ratio of the response levels of the circuit following a high-level stimulus to those achieved under no stimulus), which must reach certain levels for a cell to perform particular biological functions. We tested if the investigated regulatory circuits were responsive in the broad ranges of the rates at which the connector–target complex forms and dissociates. The calculated activation ratios for the four investigated circuits (Fig. 1) revealed that they vary with the minimal ratio exceeding 8 (Fig. 4e–h). The

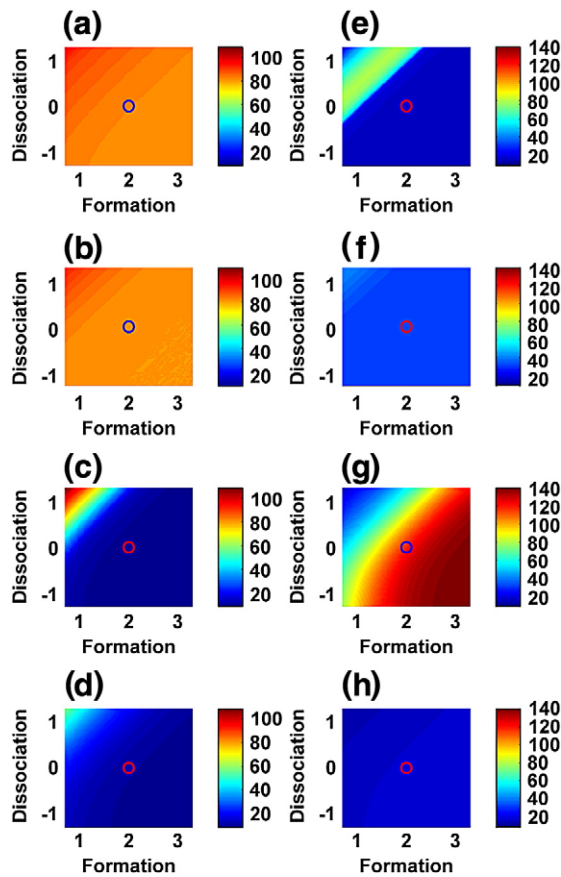


Fig. 4. Heat maps for parameter scans with the connector–target complex formation and dissociation rates varied, and other model parameters retaining their nominal values. The x -axis of each subplot corresponds to the decimal logarithm of the connector–target complex formation rate; the y -axis corresponds to the decimal logarithm of the complex dissociation rate. The circles designate nominal values of the connector–target complex formation and dissociation rates. (a–d) Deactivation times (in minutes) for the regulator-protecting circuit (a), regulator-activating circuit (b), phosphatase-inhibiting circuit (c), and kinase-stimulating circuit (d). (e–h) Activation ratios for the regulator-protecting circuit (e), regulator-activating circuit (f), phosphatase-inhibiting circuit (g), and kinase-stimulating circuit (h). Deactivation trajectories used to plot (a–d) and activation trajectories used to plot (e–h) were generated in a similar way to those displayed in Fig. 2. Deactivation times in (a–d) were calculated at the 10% level. Activation ratios in (e–h) were calculated as the output level at the trajectory end point (150 min) divided by the output level at the start point (0 min). For each parameter set, deactivation and activation of the systems were done as in the computational experiment illustrated by Fig. 2a.

minimal deactivation ratio (i.e., the ratio of the response levels achieved under a high-level stimulus to those following a decrease in stimulus) for the deactivation trajectories used to generate Fig. 4a–d exceeded 5. These results demonstrated that the connector–target complex formation and dissociation rates used in the parameter scans define responsive regulatory circuits. This suggests that

both sensor-targeting circuits and regulator-targeting circuits can perform their biological functions for a broad range of the kinetic parameters governing the interaction between a connector and its target.

Response acceleration is preserved under parameter randomizations

Our analysis indicated that response acceleration is robust to variations in certain biochemical parameters of the connector-mediated circuits (Figs. 2a, 3, and 4a–d). Thus, we wanted to explore whether response acceleration was robust under arbitrary variations in all of the circuit parameters. We tested this notion by randomizing the parameters of the circuit models (see [Supplementary Data](#) for algorithmic details). For every circuit, the sampled parameter sets were used to calculate activation and deactivation times, which, in turn, allowed us to estimate the corresponding survival functions. (The survival function $F(t)$ for activation time a is the probability that $a \geq t$, where $t \geq 0$ represents time. Similarly, the survival function for deactivation time d is the probability that $d \geq t$).

The probability of large deactivation times is significantly higher for the regulator-targeting circuits than for the sensor-targeting circuits (Fig. 5a). This implies that the response acceleration displayed by the sensor-targeting circuits is a robust dynamic property, and that this property can be attributed, to a large extent, to the mechanism of connector action. By contrast, the probability of long activation times exhibited by the phosphatase-inhibiting circuit did not exceed 0.3, indicating that the long activation delay is not robust (Fig. 5b). This result implies that the parameter randomization procedure was sufficiently thorough to filter out prominent, albeit non-robust, response timing features even if such features could be observed for the nominal parameter set. Notably, for the regulator-targeting circuits and for the kinase-stimulating circuit the probability of large activation times is even smaller, implying that all four circuits are typically characterized by rapid activation (Fig. 5b).

Deactivation dynamics of connector-mediated circuits depend on the sensor-to-regulator ratio and the degradation rate of the connector–target complex

The robust response acceleration exhibited by the sensor-targeting circuits prompted us to investigate the origin of this dynamic feature. Our computations showed that the level of connector–target complex for the regulator-protecting circuit is much higher, and the decay upon deactivation is much slower than that for the sensor-targeting circuits (Fig. 5c). This discrepancy could be a consequence of the increased abundance of the regulator compared with that of the sensor, which has been reported to be more than one order of magnitude for certain systems,^{19,20} and was implemented in our models. Thus, we posited that an increase in the abundance

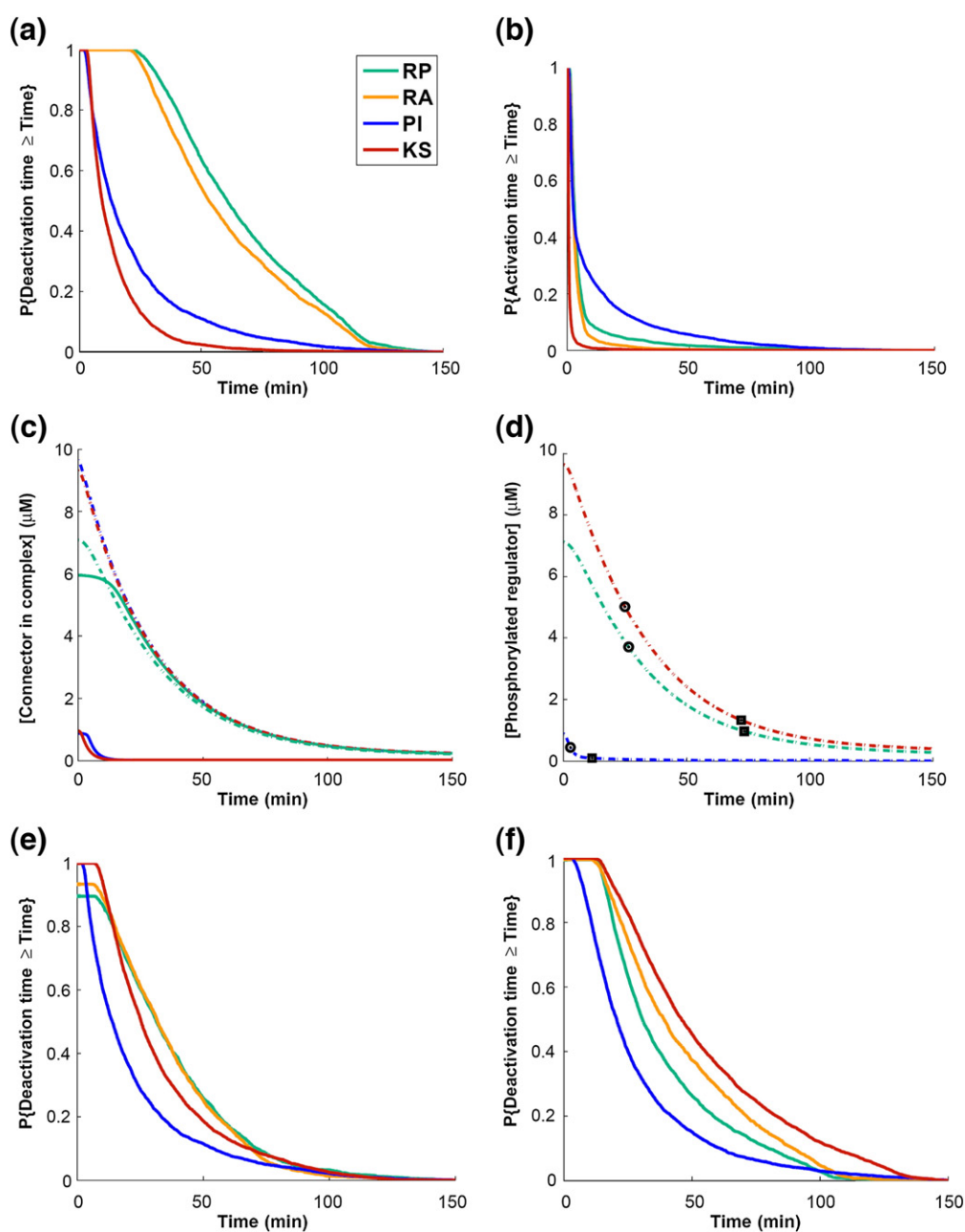


Fig. 5. Robustness of response acceleration and its dependency on the sensor-to-regulator ratio. RP, regulator-protecting circuit (Fig. 1a); RA, regulator-activating circuit (Fig. 1b); PI, phosphatase-inhibiting circuit (Fig. 1c); KS, kinase-stimulating circuit (Fig. 1d). (a and b) Deactivation time (a) and activation time (b) distributions for the connector-mediated circuits. The symbol P denotes probability. The distributions were estimated using model trajectories generated in a way similar to those displayed in Fig. 2. Each trajectory corresponded to a randomly generated parameter set. Parameter values were sampled uniformly from intervals that included the nominal parameter values; the difference between the left and right interval boundaries was approximately 10-fold (see Supplementary Data). For each parameter set, deactivation and activation of the systems were performed as in the computational experiment illustrated by Fig. 2a. The regulator-to-sensor ratio was controlled at the level of degradation, and the degradation rates for the connector-target complex were set equal to those of the targets (sensor or regulator). (c and d) Deactivation dynamics for the regulator-protecting, phosphatase-inhibiting, and kinase-stimulating circuits with the sensor protein half-life increased 10-fold. The behavior of the regulator-activating circuit is not shown. (c) Dynamics of the connector bound in complex; (d) dynamics of the phosphorylated regulator. At time zero, the connector synthesis rate was instantaneously decreased 50-fold. Continuous lines, dynamics for nominal parameter values. Dash-dot lines, dynamics with sensor half-life set equal to that of the regulator; all other parameters retained their nominal values. Filled squares mark the points that correspond to 10% activation and deactivation times; filled circles mark the points that correspond to 50% activation and deactivation times. (e and f) Deactivation time distributions for the modified connector-mediated circuits. The results were obtained in an analogous way to those shown in a. (e) The sensor-to-regulator ratio is controlled at the level of degradation, but the degradation rate of the connector-sensor complex is equal to that of the connector-regulator complex. (f) The sensor-to-regulator ratio is controlled at the level of translation.

of the sensor protein would result in higher levels of the connector–target complex and, as a consequence, lack of response acceleration in the sensor-targeting circuits. To test this notion, we modified the model by increasing the half-life of the sensor, setting it equal to the half-life of the response regulator. This resulted in comparable levels of the connector–target complex in the regulator-protecting, phosphatase-inhibiting, and kinase-stimulating circuits (Fig. 5c), and promoted expression persistence in the kinase-stimulating circuit dynamics (Fig. 5d). This effect indicates that the small sensor-to-regulator ratio is critical for the differences in expression persistence between the regulator-protecting and kinase-stimulating circuits.

The effect that an increase in the sensor half-life has on the output of a system depends on the mechanism of action of a sensor-targeting connector. This is because, in contrast to what happens with the kinase-stimulating circuit, deactivation of the phosphatase-inhibiting circuit was still rapid when the half-life of the sensor protein was increased (Fig. 5d). This was correlated with a noticeable decrease in the activated circuit output level (Fig. 5d). Such an effect can be attributed to the fact that, when the half-life of the sensor protein was increased, the accompanying increase in the concentration of the phosphatase form of the sensor protein exceeded that of the kinase form by 10-fold (Supplementary Data Fig. S1). (For the regulator-protecting and kinase-stimulating circuits, the increases in the kinase and phosphatase forms are more balanced (Supplementary Data Fig. S1).) Cumulatively, our results indicate that response acceleration displayed by the sensor-targeting circuits is due to both the specific sensor-to-regulator ratio and the particular mechanism by which a connector functions.

The degradation rate of the connector–target complex in the models is tied to the degradation rate of the connector’s target (sensor or regulator). Therefore, the sensor-to-regulator ratio, determined by the sensor and regulator degradation rates (though it could arise as a result of differential translation of the corresponding open reading frames), could exert its influence on response acceleration through the difference between the degradation rates of the connector–sensor and connector–regulator complexes. To test this, we performed parameter randomization experiments with modified models, in which the connector–sensor and connector–regulator complexes were equally stable. These experiments demonstrated a lack of significant response acceleration for sensor-targeting circuits in comparison with regulator-targeting circuits (Fig. 5e), which suggests that the difference in stability between sensor–connector and regulator–connector complexes is a critical determinant of response acceleration.

Besides a difference between the sensor and regulator degradation rates, the particular sensor-to-regulator ratio can result from distinct protein synthesis rates for the sensor and regulator. To assess the possibility of response acceleration in

such a situation, we performed parameter randomizations for modified models of connector-mediated pathways. These models were analogous to the default models (Supplementary Data Eqs (1)–(25)), but the rate of synthesis of the sensor was 10-fold less than that of the regulator; furthermore, the degradation rates for the sensor and the regulator were the same. Our analysis demonstrated the lack of response acceleration for this mechanism, because all four connector-mediated circuits generated considerable deactivation delays with probability $P > 0.5$ (Fig. 5f). We thus conclude that response acceleration is a distinct property of connector-regulated systems with sensor-to-regulator ratio controlled primarily at the level of protein degradation.

The connector-mediated architectures exhibit similar steady-state noise properties

The dynamics of genetic regulatory circuits in single cells are characterized by intrinsic stochasticity (frequently referred to as genetic noise), which arises from random behavior of molecules and relatively low abundance of regulatory proteins in a cell.^{27,28} In general, two different circuits will differ in the ability to suppress or amplify noise-induced fluctuations in the circuit response. Our analysis has shown that response timing is strongly influenced by the mechanism of connector action, whereas response levels are primarily determined by the kinetic parameters. To investigate how the magnitude of genetic noise depends on the target and mechanism of connector action, we modeled genetic noise in the regulator-and sensor-targeting circuits by using the formalism of stochastic differential equations²⁹. We numerically solved the stochastic model equations for the nominal parameter values, and calculated the steady-state response level distributions for the four circuits before and after activation (Supplementary Data Fig. S2). To characterize the degree of stochasticity in the output levels, we estimated coefficients of variation for the distributions (Table 1). These results demonstrated that the sensor-targeting and regulator-targeting circuits generate responses with similar degree of stochasticity, despite the significant discrepancies in the connector action mechanism.

Table 1. Steady-state coefficients of variation for the outputs (phosphorylated regulator concentrations) of the regulator-protecting (RP), regulator-activating (RA), phosphatase-inhibiting (PI), and kinase-stimulating (KS) circuits

	RT	RA	PI	KS
Deactivated state	0.091	0.233	0.239	0.134
Activated state	0.019	0.077	0.022	0.017

The deactivated state of the system corresponds to the nominal parameter set (Supplementary Data Table S1); the activated state corresponds to the connector synthesis rate increased 50-fold in comparison with its nominal value (all other parameter values retained their nominal values).

Discussion

Theoretical and experimental studies have demonstrated that the architecture of genetic regulatory circuits has a strong impact on the quantitative properties of the circuit.^{7,14,16,17,24,30–35} While the dynamic behavior of most circuits depends on the numerical values of the kinetic parameters, the contribution of architecture to dynamics can be elucidated by comparing the circuit behavior when the parameter values are varied, e.g. as a result of random sampling from realistic parameter ranges.^{15,25,36–38} Here, we applied systematic parameter variations (i.e., parameter scans) and parameter randomizations to compare the dynamic behavior of post-translational regulation mechanisms relying on protein–protein interactions.

Protein–protein interactions have a central role in genetic regulatory circuits.^{1,3,39–42} We have now examined the response timing properties of regulatory circuits involving TCSs and connector proteins that differ in the target and mechanism of action of the connector protein. We demonstrated that differences in the target of connector action result in distinct quantitative features of connector-mediated circuits because: (i) sensor-targeting circuits exhibit accelerated deactivation response in comparison to the regulator-targeting circuits (Figs. 2a and 5a); (ii) response acceleration is insensitive to the presence of positive autoregulation in the circuits (Fig. 2a), and is preserved when the steady-state activated response levels of the circuits are fine-tuned to attain the same values (Fig. 3); and (iii) response acceleration is robust to variations in model parameter values (Fig. 5a), particularly under wide-range variations in the connector–target complex formation and dissociation rates (Fig. 4a–d). While response acceleration is robust under parameter variations, it depends on the degradation properties of the connector–target complex (Fig. 5a and e) and on the mechanism of the sensor-to-regulator ratio control (Fig. 5a and f).

While activation can be delayed for some parameter values (Fig. 2b), activation response times for sensor-targeting circuits and for regulator-targeting circuits are typically short (Fig. 5b). This feature is common to post-translational regulatory mechanisms, because their response timing is determined primarily by the rate of covalent modification of the regulatory proteins, which is fast in comparison with transcription and translation.^{40,43} By contrast, response duration patterns in post-translationally-regulated circuits demonstrate considerable diversity, including bimodal response duration and oscillatory behavior of the mammalian global regulator NF- κ B,⁴⁴ the mammalian tumor suppressor p53,³⁹ and the cell-cycle regulator CtrA from the bacterium *Caulobacter crescentus*.⁴¹

Response duration is determined by how quickly a system is deactivated after its activating signal disappears. The simplest regulatory circuit where a TF directly controls its target genes can be deactivated within just a few minutes upon removal of its activating signal.^{14,15} Post-translational control

mechanisms, by contrast, often increase response duration due to significant half-lives of the protein complexes involved⁹ and/or special structure of the regulatory circuits.⁴⁴ For example, the strong expression persistence predicted for regulator-protecting circuits (Fig. 5a) has been established experimentally for the PmrD connector protein, which targets the TF PmrA both in *S. enterica* and *Klebsiella pneumoniae*.^{14,15} This is not unique to bacterial circuits because the TF NF- κ B, which regulates genes with critical roles in stress response, cellular growth, and apoptosis in mammalian cells,^{44,45} is inhibited by the I κ B protein, which, in turn, is regulated by phosphorylation in response to a wide variety of signals. A remarkable feature of the NF- κ B system is its ability to promote expression persistence when the system is activated by short-lasting stimuli: for instance, when the stimulus is present for 5–40 min, the response duration does not depend on the stimulus duration and equals ~ 50 min.⁴⁴ And for long-lasting stimuli, the activity of NF- κ B lasts ~ 20 min longer than the stimulus.⁴⁴

Our computations indicate that connector-mediated mechanisms targeting sensor proteins are capable of fast on-and off-switching (Fig. 5). This suggests that the duration of a response to a transient stimulus in such circuits will be comparable to the duration of the stimulus. By contrast, the response duration will be significantly longer for the regulator-targeting circuits because of their strong expression persistence. We established that, if the sensor-to-regulator ratio is controlled at the level of translation, the response timing properties depend primarily on one particular circuit feature, i.e. the target of connector action, which can impact a circuit even if all other circuit components stay the same. This is in contrast to many well-studied bacterial (e.g., CtrA⁴¹) and eukaryotic (e.g., NF- κ B^{44,45} and p53³⁹) regulatory systems, where the timing properties appear to depend on multiple network features. Moreover, our study supports the notion that a single modification in a regulatory circuit can lead to considerable differences in expression dynamics.

The deactivation dynamics of connector-mediated circuits are critically dependent on the sensor-to-regulator ratio because an increase in this ratio can abrogate response acceleration or decrease the functionality of a circuit (Fig. 5d). This suggests that connector-mediated circuits are fine-tuned to operate under the specific settings present in living cells. Increased abundance of the regulator relative to the sensor was reflected in our parameter randomization experiments, which demonstrated robustness of response acceleration under various parameters. Therefore, even relatively small biological circuits with a simple structure can possess robust quantitative properties and, thus, serve as reliable modules for regulatory networks of greater complexity. Our approach provides a general methodology for the identification of robust quantitative properties of regulatory systems, and may be applicable to other signal transduction, gene

regulation, and metabolic networks (see Ref. [46] for alternative strategies of robustness analysis in biological models).

It has been argued that the architecture and parameters of bacterial genetic circuits correlate with the circuits' functional role(s) contributing to bacterial survival in particular niches.⁴⁷ This suggests that the quantitative features of connector-mediated circuits may be related to their specific physiological functions. For example, our modeling results imply that sensor-targeting circuits are unlikely to display strong expression persistence (Fig. 5a). In this context, it is interesting that the regulator-targeting circuits mediated by the connector protein PmrD in *S. enterica* and *K. pneumoniae* promote expression persistence, and thus could contribute to the ability of these species to survive in soil,^{14,15} which is considered an unstable environment.²³ Furthermore, analysis of the genetic noise properties displayed by the various circuits revealed a similar degree of stochasticity, despite the significant differences in the connector action mechanism (Table 1 and Supplementary Data Fig. S2).

The conclusions reached on the basis of our computational studies can be tested directly in laboratory experiments with regulatory circuits involving connector proteins or other regulators acting at the post-translational level. Moreover, the modeling predictions can facilitate hypothesis generation, thereby guiding further experimentation. For example, if it is known that a bacterial species harbors a kinase-stimulating circuit (Fig. 1d), in which sensor-to-regulator ratio is controlled at the level of translation, then our model predicts that such a circuit will likely exhibit considerable deactivation delays (Fig. 5f). If its deactivation is in fact rapid, it is reasonable to hypothesize that the sensor-to-regulator ratio is controlled at the level of degradation (Fig. 5a). Because the deactivation timing characteristics are robust to parameter variations (Fig. 5a and f), we can expect that these characteristics will be observed for many of the bacterial strains belonging to the same species that harbors the regulatory circuit in question. This type of analysis could be performed, for instance, for the B1500 connector protein of *E. coli*, which stimulates the activity of the PhoP/PhoQ two-component system by targeting the sensor PhoQ.¹³ It is important to emphasize, however, that our predictions involving parameter randomizations (Fig. 5a, b, e, and f) are statistical in their nature: they might not be confirmed for a particular implementation of a genetic circuit, but will hold for a large fraction of a group of circuits with the same architecture, possibly with different parameter values. Precise characterization of the dynamics of a particular circuit can be obtained when both the architecture and parameter values for the corresponding biochemical reactions are known (Figs. 2–4).

Finally, bacterial genetic networks controlling the expression of virulence determinants can serve as targets for antimicrobial drugs.⁴⁸ A potential drug can bind with one of the proteins constituting such a

network and inhibit its activities, thereby preventing activation of the downstream virulence genes. As demonstrated for a murine model of *S. enterica* infection, virulence can depend critically on the activation dynamics of virulence determinants rather than their steady-state levels.⁶ Therefore, it is necessary to develop therapeutic strategies ensuring that the interaction of the drug with its target(s) will bring about a dynamic response with specified quantitative properties. By using approaches and techniques similar to those utilized in this work, one could make a testable prediction as to which target(s) should be inhibited to guarantee the fastest and strongest response.

Methods

The analyses presented here were done using mathematical modeling methodologies. The deterministic models of the regulator-targeting, phosphatase-inhibiting, and kinase-stimulating connector-mediated circuits are systems of ordinary differential equations that describe the concentrations of the main biochemical components of the circuits: the sensor protein in its kinase and phosphatase forms, the response regulator in its unphosphorylated and phosphorylated forms, the connector, and the connector-target complex (Supplementary Data Eqs (1)–(25)). The stochastic models of the circuits are systems of stochastic differential equations derived from the ordinary differential equations. The chemical reactions are modeled using mass action kinetics, and transcriptional control is described with sigmoidal functions.^{8,14,15} All computations were performed in MATLAB R2007a (MathWorks, Natick, MA). The details about computational procedures are given in the Supplementary Data.

Acknowledgements

We thank James Faeder, Michael Laub and Eric Siggia for comments on the manuscript. This research was supported, in part, by grant AI49561 from the National Institutes of Health to E.A.G., who is an investigator of the Howard Hughes Medical Institute.

Supplementary Data

Supplementary data associated with this article can be found, in the online version, at [doi:10.1016/j.jmb.2009.11.043](https://doi.org/10.1016/j.jmb.2009.11.043)

References

1. Freiman, R. N. & Tjian, R. (2003). Regulating the regulators: lysine modifications make their mark. *Cell*, **112**, 11–17.
2. Khidekel, N. & Hsieh-Wilson, L. C. (2004). A 'molecular switchboard' – covalent modifications to proteins and their impact on transcription. *Org. Biomol. Chem.* **2**, 1–7.

3. Mitrophanov, A. Y. & Groisman, E. A. (2008). Signal integration in bacterial two-component regulatory systems. *Genes Dev.* **22**, 2601–2611.
4. Stock, A. M., Robinson, V. L. & Goudreau, P. N. (2000). Two-component signal transduction. *Annu. Rev. Biochem.* **69**, 183–215.
5. Hoch, J. A. (2000). Two-component and phosphorelay signal transduction. *Curr. Opin. Microbiol.* **3**, 165–170.
6. Shin, D. & Groisman, E. A. (2005). Signal-dependent binding of the response regulators PhoP and PmrA to their target promoters in vivo. *J. Biol. Chem.* **280**, 4089–4094.
7. Mitrophanov, A. Y. & Groisman, E. A. (2008). Positive feedback in cellular control processes. *BioEssays*, **30**, 542–555.
8. Mitrophanov, A. Y., Churchward, G. & Borodovsky, M. (2007). Control of *Streptococcus pyogenes* virulence: modeling of the CovR/S signal transduction system. *J. Theor. Biol.* **246**, 113–128.
9. Kato, A. & Groisman, E. A. (2004). Connecting two-component regulatory systems by a protein that protects a response regulator from dephosphorylation by its cognate sensor. *Genes Dev.* **18**, 2302–2313.
10. Tzivion, G. & Avruch, J. (2002). 14-3-3 proteins: Active cofactors in cellular regulation by serine/threonine phosphorylation. *J. Biol. Chem.* **277**, 3061–3064.
11. Wösten, M. M. S. M., Kox, L. F. F., Chamnongpol, S., Soncini, F. C. & Groisman, E. A. (2000). A signal transduction system that responds to extracellular iron. *Cell*, **103**, 113–125.
12. Soncini, F. C. & Groisman, E. A. (1996). Two-component regulatory systems can interact to process multiple environmental signals. *J. Bacteriol.* **178**, 6796–6801.
13. Eguchi, Y., Itou, J., Yamane, M., Demizu, R., Yamato, F., Okada, A. *et al.* (2007). B1500, a small membrane protein, connects the two-component systems EvgS/EvgA and PhoQ/PhoP in *Escherichia coli*. *Proc. Natl Acad. Sci. USA*, **104**, 18712–18717.
14. Kato, A., Mitrophanov, A. Y. & Groisman, E. A. (2007). A connector of two-component regulatory systems promotes signal amplification and persistence of expression. *Proc. Natl Acad. Sci. USA*, **104**, 12063–12068.
15. Mitrophanov, A. Y., Jewett, M. W., Hadley, T. J. & Groisman, E. A. (2008). Evolution and dynamics of regulatory architectures controlling polymyxin B resistance in enteric bacteria. *PLoS Genet.* **e1000233**, 4.
16. Mangan, S. & Alon, U. (2003). Structure and function of the feed-forward loop network motif. *Proc. Natl Acad. Sci. USA*, **100**, 11980–11985.
17. Rosenfeld, N. & Alon, U. (2003). Response delays and the structure of transcription networks. *J. Mol. Biol.* **329**, 645–654.
18. Shin, D., Lee, J., Huang, H. & Groisman, E. A. (2006). A positive feedback loop promotes transcription surge that jump-starts *Salmonella* virulence circuit. *Science*, **314**, 1607–1609.
19. Cai, S. J. & Inouye, M. (2002). EnvZ-OmpR interaction and osmoregulation in *Escherichia coli*. *J. Biol. Chem.* **277**, 24155–24161.
20. Miyashiro, T. & Goulian, M. (2008). High stimulus unmasks positive feedback in an autoregulated bacterial signaling circuit. *Proc. Natl Acad. Sci. USA*, **105**, 17457–17462.
21. Kremling, A., Heermann, R., Centler, F., Jung, K. & Gilles, E. D. (2004). Analysis of two-component signal transduction by mathematical modeling using the KdpD/KdpE system of *Escherichia coli*. *Biosystems*, **78**, 23–37.
22. Isaacs, F. J., Hasty, J., Cantor, C. R. & Collins, J. J. (2003). Prediction and measurement of an autoregulatory genetic module. *Proc. Natl Acad. Sci. USA*, **100**, 7714–7719.
23. Hamoen, L. W., Venema, G. & Kuipers, O. P. (2003). Controlling competence in *Bacillus subtilis*: shared use of regulators. *Microbiology*, **149**, 9–17.
24. Savageau, M. A. (1974). Comparison of classical and autogenous systems in inducible operons. *Nature*, **252**, 546–549.
25. Alves, R. & Savageau, M. A. (2000). Extending the method of mathematically controlled comparison to include numerical comparisons. *Bioinformatics*, **16**, 786–798.
26. El-Samad, H. & Khammash, M. (2006). Regulated degradation is a mechanism for suppressing stochastic fluctuations in gene regulatory networks. *Biophys. J.* **90**, 3749–3761.
27. Kaern, M., Elston, T. C., Blake, W. J. & Collins, J. J. (2005). Stochasticity in gene expression: From theories to phenotypes. *Nat. Rev., Genet.* **6**, 451–464.
28. Raser, J. M. & O’Shea, E. K. (2005). Noise in gene expression: Origins, consequences, and control. *Science*, **309**, 2010–2013.
29. Higham, D. J. (2008). Modeling and simulating chemical reactions. *SIAM Rev.* **50**, 347–368.
30. Alon, U. (2007). Network motifs: theory and experimental approaches. *Nat. Rev., Genet.* **8**, 450–461.
31. Hooshangi, S., Thiberge, S. & Weiss, R. (2005). Ultrasensitivity and noise propagation in a synthetic transcriptional cascade. *Proc. Natl Acad. Sci. USA*, **102**, 3581–3586.
32. Rosenfeld, N., Elowitz, M. B. & Alon, U. (2002). Negative autoregulation speeds the response times of transcription networks. *J. Mol. Biol.* **323**, 785–793.
33. Savageau, M. A. (1975). Significance of autogenously regulated and constitutive synthesis of regulatory proteins in repressible biosynthetic systems. *Nature*, **258**, 208–214.
34. Savageau, M. A. (1976). *Biochemical Systems Analysis. A Study of Function and Design in Molecular Biology* Addison-Wesley, Reading, MA.
35. Gardner, T. S., Cantor, C. R. & Collins, J. J. (2000). Construction of a genetic toggle switch in *Escherichia coli*. *Nature*, **403**, 339–342.
36. Ingolia, N. T. (2004). Topology and robustness in the *Drosophila* segment polarity network. *PLoS Biol.* **2**, 805–815.
37. Tsai, T. Y. C., Choi, Y. S., Ma, W. Z., Pomerening, J. R., Tang, C. & Ferrell, J. E. (2008). Robust, tunable biological oscillations from interlinked positive and negative feedback loops. *Science*, **321**, 126–129.
38. von Dassow, G., Meir, E., Munro, E. M. & Odell, G. M. (2000). The segment polarity network is a robust developmental module. *Nature*, **406**, 188–192.
39. Batchelor, E., Loewer, A. & Lahav, G. (2009). The ups and downs of p53: understanding protein dynamics in single cells. *Nat. Rev., Cancer*, **9**, 371–377.
40. Rothwarf, D. M. & Karin, M. (1999). The NF- κ B activation pathway: a paradigm in information transfer from membrane to nucleus. *Science STKE*, **re1**.
41. Shen, X. L., Collier, J., Dill, D., Shapiro, L., Horowitz, M. & McAdams, H. H. (2008). Architecture and inherent robustness of a bacterial cell-cycle control system. *Proc. Natl Acad. Sci. USA*, **105**, 11340–11345.
42. Weinmaster, G. & Kintner, C. (2003). Modulation of Notch signaling during somitogenesis. *Ann. Rev. Cell Dev. Biol.* **19**, 367–395.
43. Oren, M. (1999). Regulation of the p53 tumor suppressor protein. *J. Biol. Chem.* **274**, 36031–36034.

44. Hoffmann, A., Levchenko, A., Scott, M. L. & Baltimore, D. (2002). The I κ B-NF- κ B signaling module: Temporal control and selective gene activation. *Science*, **298**, 1241–1245.
45. Hoffmann, A., Natoli, G. & Ghosh, G. (2006). Transcriptional regulation via the NF- κ B signaling module. *Oncogene*, **25**, 6706–6716.
46. Marino, S., Hogue, I. B., Ray, C. J. & Kirschner, D. E. (2008). A methodology for performing global uncertainty and sensitivity analysis in systems biology. *J. Theor. Biol.* **254**, 178–196.
47. Tagkopoulos, I., Liu, Y. C. & Tavazoie, S. (2008). Predictive behavior within microbial genetic networks. *Science*, **320**, 1313–1317.
48. Cegelski, L., Marshall, G. R., Eldridge, G. R. & Hultgren, S. J. (2008). The biology and future prospects of antivirulence therapies. *Nat. Rev. Microbiol.* **6**, 17–27.